Structure and function of the cerebral cortex in Huntington's disease

Coppen, E.M.

2

Grey matter volume loss is associated with specific clinical motor signs in **Huntington's disease**

Emma M. Coppen *, Milou Jacobs *,
Annette A. van den Berg-Huysmans,
Jeroen van der Grond, Raymund A.C. Roos

Parkinsonism and Related Disorders. 2018 Jan; 46:56-61

*These authors contributed equally

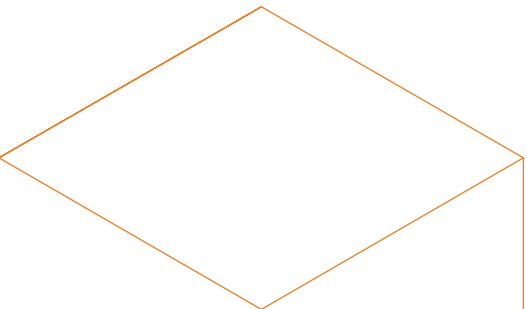

ABSTRACT

Background: Motor disturbances are clinical hallmarks of HD and involve chorea, dystonia, hypokinesia and visuomotor dysfunction. Investigating the association between specific motor signs and different regional volumes is important to understand the heterogeneity of HD.

Objectives: To investigate the motor phenotype of Huntington's disease (HD) and associations with subcortical and cortical grey matter volume loss.

Methods: Structural T1-weighted MRI scans of 79 HD patients and 30 healthy controls were used to calculate volumes of seven subcortical structures including the nucleus accumbens, hippocampus, thalamus, caudate nucleus, putamen, pallidum and amygdala. Multiple linear regression analyses, corrected for age, gender, CAG, MRI scan protocol and normalized brain volume, were performed to assess the relationship between subcortical volumes and different motor subdomains (i.e., eye movements, chorea, dystonia, hypokinesia/rigidity and gait/balance). Voxel-based morphometry analysis was used to investigate the relationship between cortical volume changes and motor signs.

Results: Subcortical volume loss of the accumbens nucleus, caudate nucleus, putamen, and pallidum were associated with higher chorea scores. No other subcortical region was significantly associated with motor symptoms after correction for multiple comparisons. Voxel-based cortical grey matter volume reductions in occipital regions were related with an increase in eye movement scores.

Conclusion: In HD, chorea is mainly associated with subcortical volume loss, while eye movements are more related to cortical volume loss. Both subcortical and cortical degeneration has an impact on motor impairment in HD. This implies that there is a widespread contribution of different brain regions resulting in the clinical motor presentation seen in HD patients.

1. INTRODUCTION

Huntington's disease (HD) is an autosomal-dominant, neurodegenerative disorder characterized by progressive motor disturbances, cognitive impairment and psychiatric symptoms. The clinical diagnosis of HD is based on the presence of motor signs, and can involve chorea, dystonia and/or hypokinesia.[1] Oculomotor dysfunction, such as saccadic eye movements or gaze paralysis, can also be prominent in premanifest and early HD.[2] The clinical HD phenotype is heterogeneous and different motor signs can also co-exist.[3] Longitudinal analysis of motor signs showed that choreatic movements decrease over time, whereas hypokinetic-rigid signs slightly increase.[4] This suggests that different motor symptoms can be more pronounced during different disease stages. The Unified HD Rating Scale Total Motor Score (UHDRS-TMS)[5] is the gold standard to evaluate motor functioning in HD and establish the clinical diagnosis. Here, several motor domains including chorea, dystonia, gait, rigidity, and eye movements are examined, with higher total scores indicating more motor dysfunction.

Although striatal atrophy is the main neuropathological finding in HD, neuronal loss has been identified in many other extrastriatal brain regions.[6] In these regions, it has been shown that grey matter volume reductions may also be associated with decreased global motor and functional scores.[7–11]

Instead of focusing on global motor functioning, we aimed to investigate associations between separate motor domains and grey matter volume changes. To monitor HD signs in clinical practice and intervention trials, it is important to further understand the pathophysiology underlying the HD phenotype, because this can vary among patients.

2. METHODS

2.1 Participants

A total of 79 patients with manifest HD and 30 healthy controls who visited the outpatient clinic at the department of Neurology of the Leiden University Medical Center (LUMC) between January 2008 and June 2016 were included. All manifest HD had a genetically confirmed CAG repeat length of ≥39 and an UHDRS-TMS of more than 5, confirming the diagnosis and clinical motor presence of HD. The local ethical committee approved this study and written informed consent was obtained from all participants.

Distinctive items of the UHDRS motor scale were added for each participant to establish total scores per motor subdomain based on previous studies,[4,12,13] representing five domains of motor functioning. For further details, see supplementary Table S1.

2.2 MRI image acquisition

All participants underwent MRI scanning on a 3 Tesla MRI scanner (Philips Achieva, Best, the Netherlands). For each participant, a structural three-dimensional T1-weighted image was acquired. Imaging parameters of the scan protocols were: TR = 7.7 ms, TE = 3.5 ms, flip angle = 8 °, FOV 24 cm, matrix size 224 x 224 cm and 164 sagittal slices to cover the entire brain with a slice thickness of 1.0 mm with no gap between slices. This resulted in a voxel size of 1,07 mm x 1,07 mm x 1,0 mm.

2.3 Image post-processing

Functional Magnetic Resonance Imaging of the Brain (FMRIB) Software Library (FSL, version 5.0.8, Oxford, United Kingdom) was used for data analysis of all structural T1-weighted images.[14] Brain tissue volume, normalized for individual head size, was estimated with SIENAX.[15] Using SIENAX, brain and skull images were extracted from the single whole-head input data. Then, the brain image is affine-registered to Montreal Neurological Institute (MNI) 152-space standard image,[16] using the skull image to determine the registration scaling. This volumetric scaling factor was used to normalize for head size. Next, tissue-type segmentation with partial volume estimation was performed in order to calculate the total volume of normalized brain tissue, including separate estimates of volumes of grey matter, white matter, peripheral grey matter and ventricular CSF for each HD patient. Visual inspection of the registration and segmentation was performed for each brain-extracted image.

2.4 Subcortical volumes

Absolute volumes of seven subcortical structures (i.e., nucleus accumbens, hippocampus, thalamus, caudate nucleus, putamen, pallidum and amygdala) were measured using FMRIB's integrated registration and segmentation tool (FIRST).[17] Here, all non-brain tissue was removed from the T1-weighted images using a semi-automated brain extraction tool that is implemented in FSL.[18] After registration of the images to the MNI 152-standard space image, using linear registration with 12° of freedom, segmentation of the subcortical regions was carried out using mesh models that were constructed from manually segmented images provided by the Center for Morphometric Analysis (CMA), Massachusetts General Hospital, Boston. Then, the volume for each structure was separately estimated. Visual inspection was performed for each output image during the registration and segmentation steps.

2.5 Voxel-based morphometry

To investigate voxel-wise differences in grey matter volume between HD patients and controls, voxel-based morphometry (VBM) analysis was performed as implemented in FSL.[19]

First, brain extracted T1-weighted images were segmented into different tissue types (i.e., grey matter, white matter or cerebrospinal fluid). Each segmented image has values that indicate the probability of a given tissue type. Then, the grey matter images were aligned to the 2 mm MNI-152 standard space image using non-linear registration. The resulting images were averaged to create a study-specific grey matter template. Subsequently, all native grey matter images were non-linearly registered to this study-specific template and 'modulated' to correct for local enlargements and contractions due to the non-linear component of the spatial transformation.[20] The modulated grey matter images were finally smoothed with an isotropic Gaussian kernel with a sigma of 3 mm and analyzed using a general linear model in FSL for statistical inference.

Brain structures that showed a significant difference between groups were identified using the Harvard-Oxford atlas integrated in FSL.

2.6 Statistical analyses

Group differences between HD patients and controls were analyzed using parametric (independent sample t-test) and non-parametric tests (χ^2-test) when applicable. To analyze group differences in the VBM output, a general linear model was constructed in FSL to compare controls with manifest HD using two-tailed t-statistics with age, gender, normalized brain volume and MRI scan protocol as covariates. Voxel-wise non-parametric permutation testing with 5000 permutations was performed using FSL randomise.[21] The Threshold-Free Cluster Enhancement (TFCE) technique was used to correct for multiple comparisons with family wise error,[22] with a p-value < 0.05 as significant threshold. The regions that showed significant differences between HD patients and controls were selected for further analyses in the HD group only.

The following analyses, investigating the relationship between separate motor subdomains, subcortical and cortical brain volumes, were performed in HD patients only. Multiple linear regression analyses were used to investigate the relationship between the separate motor subdomains and subcortical brain volumes. Analyses were accounted for age, gender, CAG repeat length, normalized brain volume, and MRI scan protocol. To correct for multiple comparisons the p-value for statistical significance was set at $p < 0.008$ (0.05/6) for analyses of subcortical volumes. To assess the relationship between clinical motor scores and cortical grey matter changes in HD patients, a general linear model was constructed using a design matrix in FSL with

each clinical motor domain separately, correcting for age, gender, CAG repeat length, normalized brain volume, and MRI scan protocol. FSL-Randomise was used for voxel-wise non-permutation testing,[21] using the regions that showed significant grey matter changes between controls and HD patients as a grey matter mask. Again, the TFCE technique was used to correct for multiple comparisons with family wise error,[22] with a p-value < 0.05 as significant threshold. Statistical analyses were performed using IBM SPSS 23.0 for Windows.

3. RESULTS

Group characteristics and comparisons between HD patients and controls are reported in Table 1. There were no significant differences in age and gender between both groups. HD patients had a significantly higher mean UHDRS-TMS compared to the control group.

3.1 Subcortical volumes

The mean volumes of the accumbens nucleus, caudate nucleus, putamen, pallidum, thalamus and hippocampus were significantly lower in manifest HD compared to controls (Table 1). Since the mean volume of the amygdala did not differ between HD patients and controls, this structure was not included in further analyses in HD patients only.

After correction for multiple comparisons, there was a significant association between the UHDRS chorea score and UHDRS-TMS with the accumbens nucleus, caudate nucleus, putamen and pallidum in HD patients (Table 2). Thalamus and hippocampus volumes did not show any association with UHDRS motor subdomains.

3.2 Cortical grey matter volume

To assess differences in cortical grey matter volume between HD patients and controls, regional volumetric VBM analysis was performed. Significant grey matter volume reduction in HD patients was found in the motor cortex, visual cortex, and in the frontal and temporal lobes (Figure 1 and supplementary Table S2).

In HD patients, VBM analysis showed that after correction for covariates and multiple comparisons, higher eye movement scores and UHDRS-TMS were associated with cortical volume loss of occipital regions (Figure 2 and supplementary Table S3).

TABLE 1 Clinical and volumetric group differences between HD patients and controls

	HD (n= 79)	Controls (n=30)	*p*-value
Clinical characteristics			
Age	46.5 (9.7; 28 – 65)	48.9 (8.4; 35 – 65)	0.229
Gender m/f (%m)	30/49 (38.0%)	14/16 (46.7%)	0.409
CAG	44.1 (2.4; 40 – 51)	NA	NA
Disease duration	3.3 (3.0; 0 – 13)	NA	NA
Disease burden	382.1 (77.8; 234 – 551)	NA	NA
UHDRS-TMS	17.8 (10.8; 6 – 45)	2.6 (2.4; 0 – 7)	**<0.001**
UHDRS chorea	5.2 (4.8; 0 – 18)	NA	NA
UHDRS hypokinetic-rigid	4.6 (3.2; 0 – 12)	NA	NA
UHDRS dystonia	0.2 (0.6; 0 – 3)	NA	NA
UHDRS eye movements	4.9 (3.2; 0 – 13)	NA	NA
UHDRS gait/balance	1.8 (1.4; 0 – 6)	NA	NA
Subcortical structures			
Accumbens nucleus	732.0 (188.0)	930.5 (207.0)	**<0.001**
Caudate nucleus	4942.2 (997.5)	6695.4 (839.0)	**<0.001**
Amygdala	2208.0 (528.5)	2163.4 (379.4)	0.673
Putamen	7093.0 (1229.1)	9280.0 (1289.7)	**<0.001**
Pallidum	2749.8 (555.8)	3338.5 (471.4)	**<0.001**
Thalamus	13958.0 (1551.3)	14844.2 (1383.7)	**<0.005**
Hippocampus	7195.4 (1016.0)	7682.1 (818.3)	**0.021**

Data are mean (SD; range) or number (%) for gender. Volumes of subcortical structures are expressed in mm^3. Mean disease duration is based on a smaller sample size (n=65) due to missing data. Independent sample t-test was used to compare groups, except for gender (χ^2-test). Statistically significant *p*-values are highlighted in bold ($p<0.05$). NA = Not applicable; CAG = Cytosine-Adenine-Guanine; HD = Huntington's Disease; UHDRS = Unified Huntington's Disease Rating Scale; TMS = Total Motor Score.

TABLE 2 Relationship between UHDRS motor subdomains and subcortical brain volumes

	Accumbens nucleus	Caudate nucleus	Putamen	Pallidum	Thalamus	Hippocampus
UHDRS-TMS	**-0.283**	**-0.316**	**-0.279**	**-0.312**	-0.096	-0.265
UHDRS chorea	**-0.260**	**-0.346**	**-0.275**	**-0.273**	-0.045	-0.172
UHDRS hypokinetic-rigid	-0.180	-0.118	-0.175	-0.156	-0.052	-0.179
UHDRS dystonia	-0.075	-0.033	-0.012	0.076	0.056	0.047
UHDRS eye movements	-0.188	-0.212	-0.171	-0.239	-0.169	-0.240
UHDRS gait/balance	-0.097	-0.056	-0.112	-0.214	-0.057	-0.245

Reported data are standardized coefficients (standardized beta) from the multiple linear regression analysis. Analyses were accounted for age, gender, CAG, MRI scan protocol, and normalized brain volume. Statistically significant values are printed in bold (corrected for multiple comparisons, $p < 0.008$). UHDRS = Unified Huntington's Disease Rating Scale; TMS = Total Motor Score

FIGURE 1 Voxel based morphometry analysis between manifest HD and controls

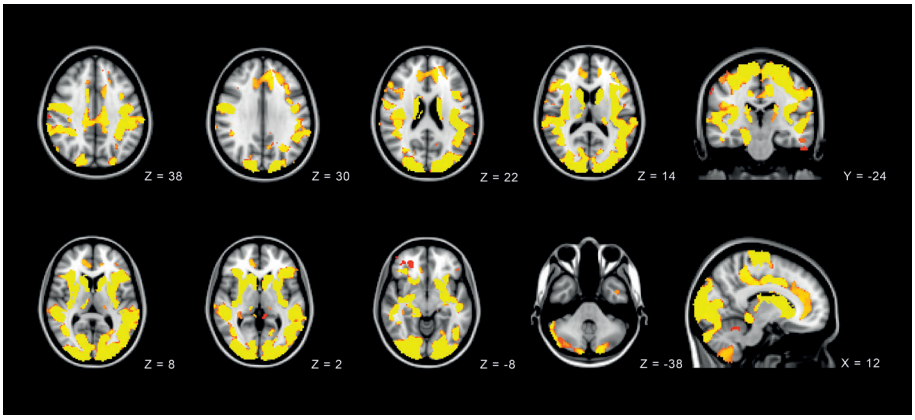

Brain regions that showed significant differences in grey matter volume in manifest HD compared to controls by means of voxel-based morphometry (VBM) are presented. Age, gender, MRI study protocol and normalized brain volume were included as covariates in the statistical model. Identified grey matter regions are overlaid on sagittal, transversal and coronal slices of Montreal Neurological Institute (MNI)-152 standard space T1-weighted images. Corresponding MNI x-, y-, z- coordinates are displayed. A threshold of $p < 0.05$ (corrected with TFCE family wise error) is used.

4. DISCUSSION

Our study showed that specific clinical motor signs in manifest HD are related to volume loss in different grey matter brain regions. Higher UHDRS chorea scores were particularly related to volume loss of subcortical structures, especially the accumbens nucleus, caudate nucleus, putamen and pallidum, whereas cortical brain regions did not. These findings suggest that volume loss in the subcortical regions are more involved in the development of chorea than cortical atrophy. It is well known that the medium-sized spiny neurons located in the striatum, that comprises of the caudate nucleus and putamen, are the most affected cells in HD.[23] As these neurons are involved in motor control, this might explain the association we found between striatal volume loss and the UHDRS chorea score.

In premanifest HD, general motor functioning is related to volume loss of the putamen, caudate nucleus and pallidum.[7,10,11] Increased choreatic movements have been associated with striatal atrophy in premanifest HD.[24] However, to our knowledge, no studies have been performed that examined motor domains separately in relation with both subcortical and cortical changes. In addition to striatal volume loss, we observed a correlation between volume loss of the pallidum and higher UHDRS chorea scores.

It is suggested that changes in the pallidum might be due to the loss of striato-pallidal fibers projecting from striatal medium spiny neurons, implying that volume loss of the pallidum is not due to cell loss within the pallidum.[11]

Besides subcortical grey matter volume changes, we also investigated the association with cortical regions in patients with HD. Here, cortical grey matter volume loss was particularly associated with oculomotor dysfunction, but not with choreatic signs. Our findings are in contrast with results reported in a previous study where no correlations were found between cortical grey matter and motor functioning in premanifest HD.[11] A possible explanation might be that this previous study calculated lobular cortical volumes instead of investigating relationships with cortical volumes using a voxel-based technique. Another explanation could be that the HD patients included in our study were in a more advanced disease stage with more motor impairments, suggesting that involvement of cortical regions is more pronounced later in the disease. Still, UHDRS dystonia and hypokinetic-rigid scores did not show any significant correlations with subcortical volumes in our study.

The motor cortex, visual cortex, and cortical regions in the frontal and temporal lobes showed significant decrease in grey matter volume in manifest HD compared to controls by means of voxel-based morphometry. These identified regions are consistent with

FIGURE 2 Correlations between clinical motor scores and grey matter loss in manifest HD

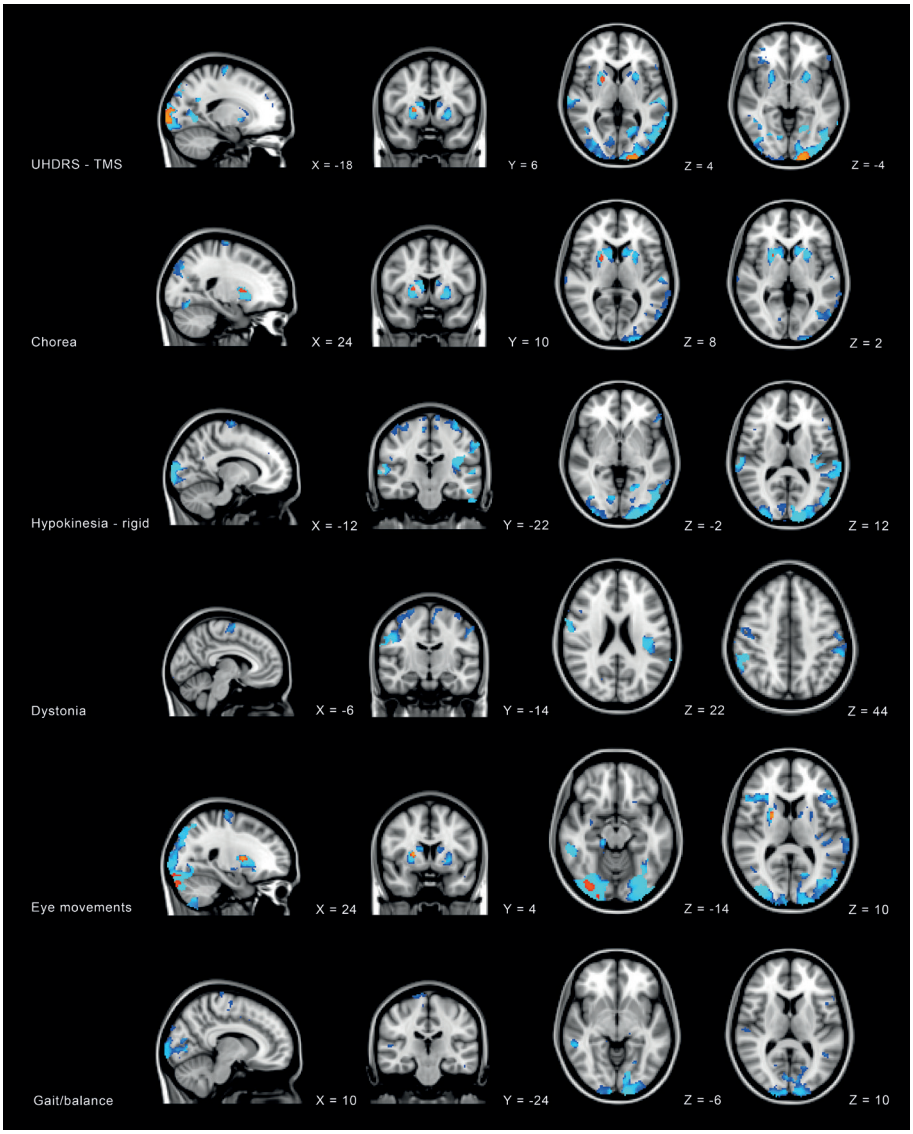

VBM analyses showing significant correlations between increased motor scores and reduction in grey matter volume. A threshold of $p < 0.05$ is used. Brain regions in blue are uncorrected for multiple testing and red-yellow brain regions are corrected with TFCE family wise error. Results are overlaid on sagittal, transversal and coronal slices of Montreal Neurological Institute (MNI)-152 standard space T1-weighted images. Corresponding MNI x-, y-, z- coordinates are displayed. UHDRS – TMS = Unified Huntington's Disease Rating Scale – Total Motor Score.

findings in previous voxel-based studies.[11,25–28] Additionally, we observed volume loss in visual cortical regions, which were associated with higher eye movement scores in HD gene carriers. It is known that fronto-striatal and occipital regions are important for oculomotor control and visual processing,[29,30] providing a possible explanation for the observed correlations in these specific motor domains. These results are comparable to other studies observing associations between volume changes and quantitative motor functioning.[27,28]

It has also been reported that more prominent bradykinesia and dystonia are related to cortical thinning of the anterior frontal regions, including the premotor and supplementary motor cortex.[9,28] In addition, finger tapping has been related to striatal and cortical atrophy.[24,28] Although we investigated changes in subcortical and cortical regions separately, there is a known interplay between the basal ganglia and cerebral cortex. Especially changes of the basal ganglia-thalamo-frontal circuits are known to contribute to hyperkinetic movements such as chorea.[11,23]

We did not find an association between some of the motor domains and grey matter regions, such as the cingulate gyrus. Since we aimed to focus on the clinical hallmark of HD, which is the presence of motor signs, this absent association might be caused by the fact that these brain regions are also involved in other domains than motor control. It has been reported that cortical brain atrophy, specifically in frontal, parietal and occipital lobes is related to a decline in cognitive functioning.[9,27,30] Future studies investigating the relationship between cognitive and psychiatric symptoms of HD and volume reductions of the brain are necessary to further understand the pathogenesis of HD.

The lack of a relationship between dystonia and subcortical volumes in our study might also be caused by the relatively low scores on this item in our cohort of early stage HD patients. A further limitation of this study is the relatively smaller sample size of the control group, which could potentially influence the results. A larger sample size of the control group is preferred in future studies.

In conclusion, patients with HD can present with a heterogeneous motor phenotype, consisting of chorea, dystonia, hypokinesia and/or balance disturbances. Our results demonstrate that chorea, which is the clinical hallmark of HD, is strongly associated with subcortical volume loss of the striatum and pallidum and not with cortical atrophy. Oculomotor dysfunction, however, seems to be more related to cortical volume changes, especially in occipital regions. Thus, there is a widespread contribution of different brain regions resulting in the overall clinical motor presentation seen in HD patients. We showed that not only subcortical volume loss is involved in the expression of motor disturbances, but also, although to a much lesser extent, cortical degeneration.

REFERENCES

1. Roos RAC. Huntington's disease: a clinical review. *Orphanet J Rare Dis*. 2010;5(1):40.
2. Blekher TM, Yee RD, Kirkwood SC, et al. Oculomotor control in asymptomatic and recently diagnosed individuals with the genetic marker for Huntington's disease. *Vision Res*. 2004;44:2729-2736.
3. Thompson P., Berardelli A, Rothwell J., et al. The coexistence of bradykinesia and chorea in Huntington's disease and its implications for theories of basal ganglia control of movement. *Brain*. 1988;111:223-244.
4. Jacobs M, Hart EP, van Zwet EW, et al. Progression of motor subtypes in Huntington's disease: a 6-year follow-up study. *J Neurol*. 2016;263(10):2080-2085.
5. Huntington Study Group. Unified Huntington's disease rating scale: reliability and consistency. *Mov Disord*. 1996;11(2):136-142.
6. de la Monte S, Vonsattel J, Richardson E. Morphometric demonstration of atrophic changes in cerebral cortex, white matter and neostriatum in Huntington's disease. *J Neuropathol Exp Neurol*. 1988;47(5):516-525.
7. Jurgens CK, van de Wiel L, van Es ACGM, et al. Basal ganglia volume and clinical correlates in "preclinical" Huntington's disease. *J Neurol*. 2008;255(11):1785-1791.
8. Gómez-Ansón B, Alegret M, Muñoz E, et al. Prefrontal cortex volume reduction on MRI in preclinical Huntington's disease relates to visuomotor performance and CAG number. *Park Relat Disord*. 2009;15(3):213-219.
9. Rosas HD, Salat DH, Lee SY, et al. Cerebral cortex and the clinical expression of Huntington's disease: complexity and heterogeneity. *Brain*. 2008;131(4):1057-1068. doi:10.1093/brain/awn025.
10. van den Bogaard SJA, Dumas EM, Acharya TP, et al. Early atrophy of pallidum and accumbens nucleus in Huntington's disease. *J Neurol*. 2011;258(3):412-420.
11. Aylward EH, Harrington DL, Mills JA, et al. Regional atrophy associated with cognitive and motor function in prodromal Huntington disease. *J Huntingtons Dis*. 2013;2:477-489.
12. Marder K, Zhao H, Myers RH, et al. Rate of functional decline in Huntington's disease. *Neurology*. 2000;54:452-458.
13. Mahant N, McCusker E., Byth K, Graham S. Huntington's disease: clinical correlates of disability and progression. *Neurology*. 2003;61:1085-1092.
14. Smith SM, Jenkinson M, Woolrich MW, et al. Advances in functional and structural MR image analysis and implementation as FSL. *Neuroimage*. 2004;23:S208-S219.
15. Smith SM, Zhang Y, Jenkinson M, et al. Accurate, robust, and automated longitudinal and cross-sectional brain change analysis. *Neuroimage*. 2002;17(1):479-489.

16. Jenkinson M, Bannister P, Brady M, Smith S. Improved optimization for the robust and accurate linear registration and motion correction of brain images. *Neuroimage*. 2002;17(2):825-841.
17. Patenaude B, Smith SM, Kennedy DN, Jenkinson M. A Bayesian model of shape and appearance for subcortical brain segmentation. *Neuroimage*. 2011;56(3):907-922.
18. Smith SM. Fast robust automated brain extraction. *Hum Brain Mapp*. 2002;17(3):143-155.
19. Ashburner J, Friston KJ. Voxel-Based Morphometry—The Methods. *Neuroimage*. 2000;11(6):805-821.
20. Good C, Johnsrude I, Ashburner J, Henson R, Friston K, Frackowiak R. A voxel-based morphometric study of ageing in 465 normal adult human brains. *Neuroimage*. 2001;14(1):21-36.
21. Winkler AM, Ridgway GR, Webster MA, Smith SM, Nichols TE. Permutation inference for the general linear model. *Neuroimage*. 2014;92:381-397.
22. Smith SM, Nichols TE. Threshold-free cluster enhancement: addressing problems of smoothing, threshold dependence and localisation in cluster inference. *Neuroimage*. 2009;44(1):83-98.
23. Reiner A, Albin RL, Anderson KD, D'Amato CJ, Penney JB, Young AB. Differential loss of striatal projection neurons in Huntington disease. *Proc Natl Acad Sci U S A*. 1988;85(15):5733-5737.
24. Biglan KM, Ross CA, Langbehn DR, et al. Motor abnormalities in premanifest persons with Huntington's disease: The PREDICT-HD study. *Mov Disord*. 2009;24(12):1763-1772.
25. Kassubek J, Juengling FD, Kioschies T, et al. Topography of cerebral atrophy in early Huntington's disease: a voxel based morphometric MRI study. *J Neurol Neurosurg Psychiatry*. 2004;75(2):213-220.
26. Tabrizi SJ, Langbehn DR, Leavitt BR, et al. Biological and clinical manifestations of Huntington's disease in the longitudinal TRACK-HD study: cross-sectional analysis of baseline data. *Lancet Neurol*. 2009;8(9):791-801.
27. Scahill RI, Hobbs NZ, Say MJ, et al. Clinical impairment in premanifest and early Huntington's disease is associated with regionally specific atrophy. *Hum Brain Mapp*. 2013;34(3):519-529.
28. Bechtel N, Scahill RI, Rosas HD, et al. Tapping linked to function and structure in premanifest and symptomatic Huntington disease. *Neurology*. 2010;75(24):2150-2160.
29. Lobel E, Kahane P, Leonards U, et al. Localization of human frontal eye fields: anatomical and functional findings of functional magnetic resonance imaging and intracerebral electrical stimulation. *J Neurosurg*. 2001;95:804-815.
30. Johnson EB, Rees EM, Labuschagne I, et al. The impact of occipital lobe cortical thickness on cognitive task performance: An investigation in Huntington's Disease. *Neuropsychologia*. 2015;79:138-146.

SUPPLEMENTARY MATERIAL

TABLE S1 Subscales of five motor domains based on the Unified Huntington's Disease Rating Scale (UHDRS)

Motor sum scores	Description	Items from UHDRS	Range
Chorea	Chorea	12	0 – 28
Dystonia	Dystonia	11	0 – 20
Eye movements	Ocular, saccades	1, 2, 3	0 – 24
Hypokinesia/rigidity	Finger tapping, pronate/supinate, bradykinesia, rigidity	6, 7, 9, 10	0 – 28
Gait/balance	Gait, tandem walking, retropulsion	13, 14, 15	0 – 12

Motor domains are based on previous studies.[5, 14, 15] Scores of each individual item of the UHDRS were summed to create the specific motor domains.
UHDRS = Unified Huntington's Disease Rating Scale

TABLE S2 Grey matter differences in manifest HD compared to controls

	MNI coordinates (mm)			t-value	*p*-value
	x	y	z		
Frontal lobe					
Precentral gyrus	14	-14	76	6.65	<0.001
Supplementary motor cortex	10	-22	66	6.17	<0.001
Frontal orbital cortex	24	42	-8	3.21	0.043
Frontal pole	36	44	-6	3.10	0.044
Temporal lobe					
Inferior temporal gyrus	48	-36	-14	6.37	<0.001
Middle temporal gyrus	-46	-58	6	6.06	<0.001
Parietal lobe					
Postcentral gyrus	-20	-34	72	3.16	<0.001
Supramarginal gyrus	66	-22	42	3.37	0.045
Cingulate gyrus	-8	-38	2	3.51	0.043
Occipital lobe					
Occipital pole	26	-92	0	7.34	<0.001
Occipital fusiform gyrus	22	-80	-10	7.11	<0.001
Lateral occipital cortex	-30	-94	4	6.91	<0.001

Anatomical regions that showed a significant difference in grey matter volume between manifest HD and controls using voxel-based morphometry. All anatomical regions were identified using the Harvard-Oxford Subcortical and Cortical atlases and the cluster tool implemented in FSL. T-statistics and corresponding *p*-values are presented (with a family wise corrected *p*-value of $p<0.05$)

TABLE S3 Correlations between anatomical regions and clinical scores in HD patients

	Anatomical region	Voxel size	MNI coordinates (mm)			t-value	*p*-value
			x	y	z		
UHDRS-TMS	Left occipital pole	403	-16	-100	-2	1.05	0.019
	Right putamen	33	22	4	6	1.47	0.024
Chorea	Right putamen	23	22	4	6	1.32	0.038
Eye movements	Lateral occipital cortex	172	20	-92	-28	0.92	0.036
	Occipital fusiform gyrus	141	32	-84	-16	0.95	0.036
	Right putamen	41	22	2	8	1.65	0.016

Voxel-wise identified anatomical regions that showed a negative correlation with clinical scores in HD patients, i.e. an increase in clinical score is correlated with a decrease in grey matter volume. All anatomical regions were identified using the Harvard-Oxford Subcortical and Cortical atlases and the cluster tool implemented in FSL. T-statistics and corresponding *p*-values are presented (with a TFCE-family wise corrected *p*-value of $p < 0.05$).

2